

# Histogram-pattern analysis of the lung perfused blood volume for assessment of pulmonary thromboembolism

Munemasa Okada 

Takafumi Nomura 

Yoshiteru Nakashima 

Yoshie Kunihiro

Shoji Kido 

## PURPOSE

We aimed to evaluate the usefulness of histograms of lung perfused blood volume ( $H_{LPBV}$ ) based on the presence of pulmonary thromboembolism (PTE) and the pulmonary embolic burden.

## METHODS

A total of 168 patients (55 males; mean age, 62.9 years) underwent contrast-enhanced dual-energy computed tomography (DECT) between January 1 2012 and October 31 2014. Initial DECT images were three-dimensionally reconstructed, and the  $H_{LPBV}$  patterns were divided into three types, including the symmetric type (131 patients, 78.0%), gradual type (25 patients, 14.9%), and asymmetric type (12 patients, 7.1%).

## RESULTS

Acute PTE was diagnosed in all 12 patients with asymmetric type (100%), 19 of the 25 patients with gradual type (76%) and 24 of the 131 patients with symmetric type (18.3%).  $H_{LPBV}$  pattern exhibited correlations with the right/left ventricular diameter ratio ( $r=0.36$ ,  $P=0.007$ ) and CT obstruction index ( $r=0.63$ ,  $P<0.001$ ) in patients with PTEs. When the gradual and asymmetric types were regarded as positive for PTE, the specificity, positive predictive value, negative predictive value, and accuracy were 92.9%, 83.8%, 87.6%, and 81.0%, respectively.

## CONCLUSION

Histogram-pattern analysis using DECT might be a useful application to diagnose PTE.

**P**ulmonary thromboembolism (PTE) is a potentially fatal disorder and is the third most common cause of acute cardiovascular disease (1). Dual-energy computed tomography (DECT) reliably depicts segmental defects in iodine distribution corresponding to embolic vessel occlusion, the D-dimer level or cardiovascular CT parameters (2–7). Attempts to evaluate the severity of pulmonary embolism with the volumetric lung perfused blood volume (LPBV) (8) or whole LPBV automatically calculated on a workstation have been reported using DECT (9). However, the injection rate of contrast material (10) and right ventricular dysfunction due to proximal intrapulmonary clot (IPC) burden also affect the pulmonary circulation and degree of pulmonary parenchymal enhancement (11), and the clinical relevance of assessing the severity of PTE by quantifying the LPBV has not been established.

The purpose of this study was to evaluate the usefulness and effectiveness of histogram-pattern analyses of the volumetric LPBV for determining the clinical severity and degree of right ventricular dysfunction based on the presence of PTE and IPC burden.

## Methods

### Patients and parameters

A total of 207 patients (75 males; mean age,  $63.3 \pm 16.1$  years) suspected of having acute PTE underwent DECT between January 1 2012 and October 31 2014. Thirty-nine patients were excluded from this study, due to pulmonary comorbidities, including severe pulmonary emphysema ( $n=10$ ), bronchopneumonia or interstitial lung diseases ( $n=14$ ), motion artifact as a result of insufficient breath-holding ( $n=6$ ), and a previous history of PTE ( $n=9$ ). The LPBV was scanned according to the dual-energy technique using dual-source CT (SOMATOM Definition, Siemens

From the Department of Radiology (M.O. ✉ [radokada@yamaguchi-u.ac.jp](mailto:radokada@yamaguchi-u.ac.jp), T.N., Y.K.) Yamaguchi University Graduate School of Medicine, Ube, Yamaguchi, Japan; Department of Radiology (Y.N.), Yamaguchi Grand Hospital, Hofu, Yamaguchi, Japan and the Department of Computer-aided Diagnosis and Biomedical Imaging Research Biomedical Engineering (S.K.), Applied Medical Engineering Science Graduate School of Medicine, Yamaguchi University, Ube, Yamaguchi, Japan.

Received 15 August 2017; revision requested 1 October 2017; last revision received 31 January 2018; accepted 1 February 2018.

Published online 19 April 2018.

DOI 10.5152/dir.2018.17311

You may cite this article as: Okada M, Nomura T, Nakashima Y, Kunihiro Y, Kido S. Histogram-pattern analysis of the lung perfused blood volume for assessment of pulmonary thromboembolism. *Diagn Interv Radiol* 2018; 24:139–145.

Healthcare) within 48 hours of symptom onset, including the development of dyspnea, chest discomfort and pain. A total of 168 patients (55 males; mean age,  $62.9 \pm 16.8$  years) were included in this study. Acute PTE was diagnosed in 55 patients (19 males; mean age,  $62.0 \pm 18.7$  years) based on laboratory data and the findings of echocardiography as well as 2 mm slice CT pulmonary angiography (CTPA) weighted average 120 kVp images showing complete, partial, or peripheral filling defects in the pulmonary arteries. Echocardiography and measurement of the D-dimer level were also performed within 24 hours before or after scanning of DECT. The LPBV images were three-dimensionally reconstructed with two thresholds ranging from 1 to 5 HU ( $V_5$ ) and 120 HU ( $V_{120}$ ) and the histogram of whole LPBV ( $H_{LPBV}$ ) was obtained using a workstation (AZE VirtualPlace™, AZE). The study protocol was approved by the local ethics committee. Informed consent for the DECT assessments was obtained individually from each patient, whereas informed consent for the retrospective volumetric CT analysis was waived.

### CT image acquisition

LPBV images were scanned using dual-source CT scanner with two X-ray tubes and corresponding detectors placed with an angular offset of  $90^\circ$ . The first detector array provided a field of view (FOV) of 50 cm, and the second one provided a smaller FOV of 26 cm with the detector collimation  $32 \times 0.6$  mm. Tube voltages and currents used were 80 kVp (200 mAs) and 140 kVp (50 mAs). The gantry rotation time was 0.5 s with pitch value of 0.5. The caudocranial scan of LPBV

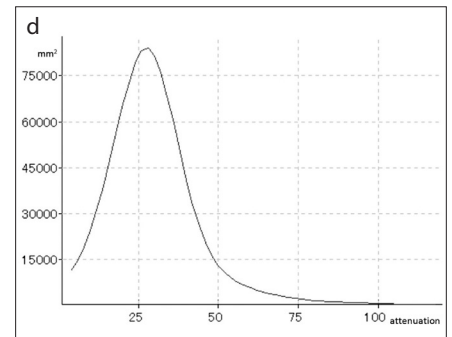
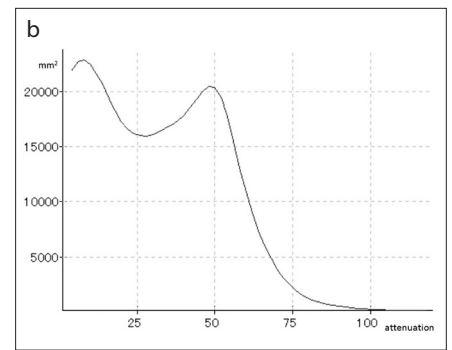
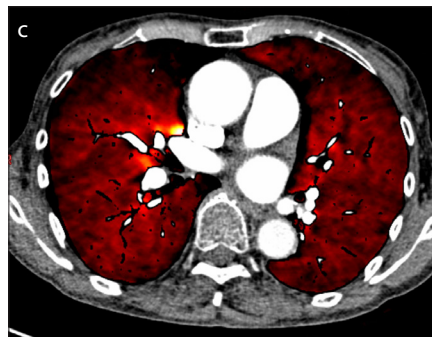
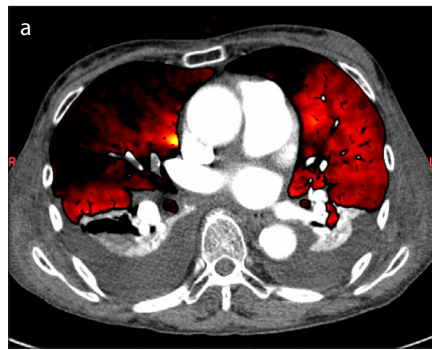


**Figure 1.** a–d. Color-coded LPBV images and histogram patterns of LPBV in a 52-year-old female patient with acute PTE. LPBV image shows multiple perfusion defects (a) and the irregular (bumpy) histogram (b). Three months after anticoagulation therapy, PTE disappeared (c) and the histogram became symmetric (d).

started using bolus tracking technique when the attenuation of the main pulmonary trunk exceeded a threshold of 100 HU following the intravenous administration of low-osmolar nonionic iodinated contrast material (body weight  $<60$  kg, 300 mgI/mL and body weight  $>60$  kg, 350 mgI/mL, Omnipaque; Daiichi-Sankyo) via a 20-gauge catheter into the antecubital vein at a rate of 4 mL/s (100 mL of pure contrast medium followed by 30 mL of saline).

### Image reconstruction

The weighted average images were approximated to 120 kVp images automatically generated from a combination of the 140 kVp and 80 kVp data using a weighting factor of 6:4. Transverse CT images were reconstructed using a soft tissue kernel (D30f), and LPBV images were generated using a workstation with postprocessing software (syngo via; Syngo Dual Energy software, Siemens Healthcare). The basic principle of DECT is material decomposition based on attenuation differences at different energy levels (14). In the lung consisting of air, soft tissue, and iodine, the algorithm assigns a ratio of air and soft tissue to the voxel; at the same time, the CT numbers at both 80 kVp and 140 kVp images are used to derive the

additional iodine content as LPBV using a three-material composition technique. The volume rendering technique was automatically applied for the three-dimensional reconstruction of the LPBV in two threshold ranges of  $V_5$  and  $V_{120}$ , and the LPBV images were extracted without the findings for the trachea or main bronchus. The whole LPBV images were defined as the  $V_{120}$  based on our experiences. The low perfusion value ( $V_5$ ) increased by the presence of PTE, and the ratio of  $V_5/V_{120}$  was expressed as  $\%V_5$ . The diameters of right ventricle (RV) and left ventricle (LV), pulmonary artery (PA)/aorta (Ao) diameter ratio were measured, and CT obstruction index (CTOI) was calculated using Qanadli method (12, 13).

### Histogram pattern analysis

In patients with PTE (Fig. 1a), the  $H_{LPBV}$  showed the irregular shape type (Fig. 1b). However, the  $H_{LPBV}$  feature became symmetric three months after anticoagulation therapy (Fig. 1c, 1d). The  $H_{LPBV}$  types were divided into three categories according to the up-slope shape of  $H_{LPBV}$ ; the symmetric (S) type with a rapid up- and down-slope angle (Fig. 2a, 2d), the gradual (G) type with a more gradual upslope than down-slope angle (Fig. 2b, 2e) and the asymmetric (A)

#### Main points

- Dual-energy computed tomography (DECT) provides iodine perfusion map in lung parenchyma as lung perfused blood volume images (LPBV).
- The histogram pattern of LPBV have correlations with the factors suggesting right heart strain, including the right/left ventricular diameter ratio ( $r=0.36, P=0.007$ ) and CT obstruction index ( $r=0.63, P<0.001$ ).
- When the histogram patterns with gradual and asymmetric types are regarded as positive for pulmonary thromboembolism, the specificity, PPV, NPV and accuracy are 92.9%, 83.8%, 87.6% and 81.0%, respectively.
- The histogram pattern of LPBV can be helpful for gross evaluation of right heart strain in patients with intrapulmonary clots.

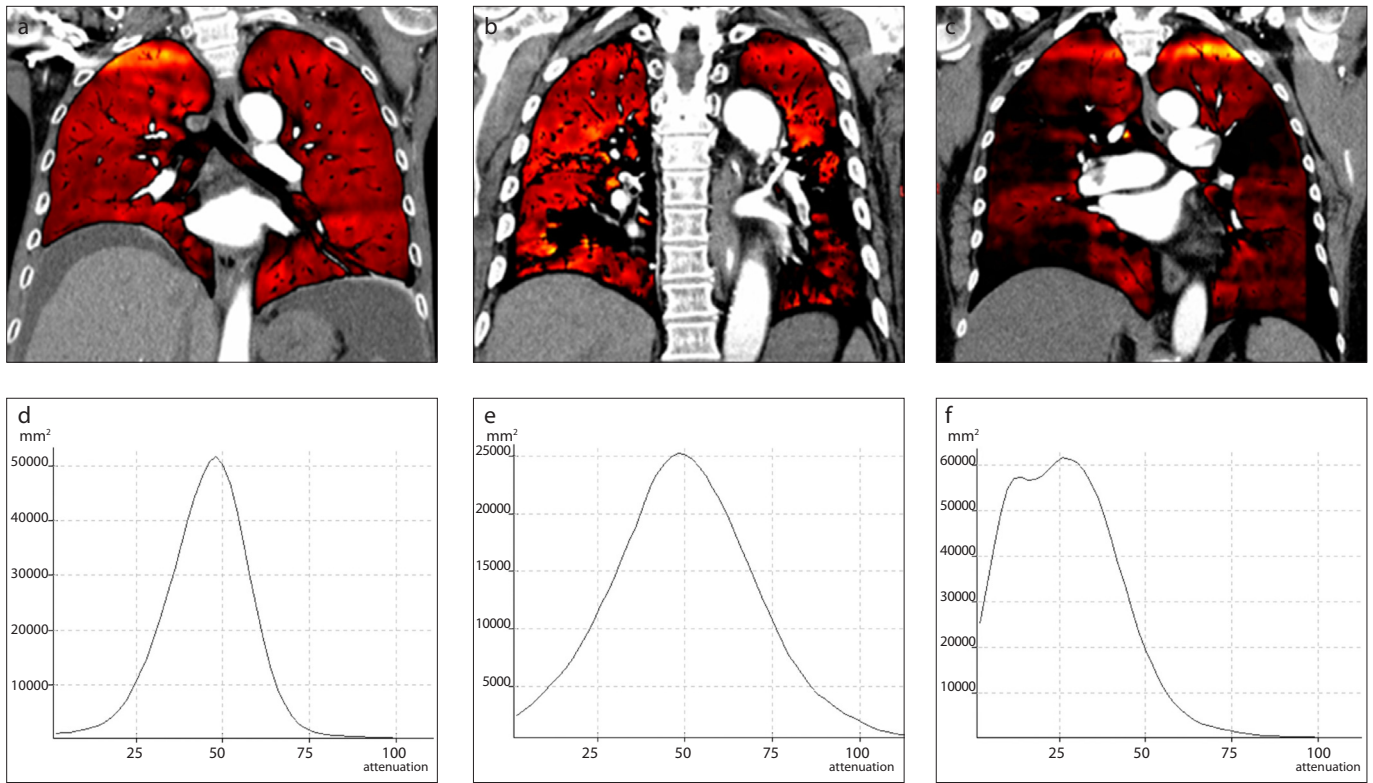


**Figure 2.** a–f. The histogram patterns of LPBV were divided into three types based on the up-slope shape (a–c). The histogram in a patient without PTE demonstrates symmetry of the up- and down-slope angles (d). The histograms of patients with PTE have more gradual up-slope angle than down-slope angle (e) and bumpy up-slopes (f).

type with a bumpy up-slope (Fig. 2c, 2f) or twin peaks. In patients with PTE, the decreased PA flow caused by IPC might lead to increase of the low attenuation volumes in LPBV meaning hypoperfusion, and the  $H_{LPBV}$  types might shift from S-type to A-type. To evaluate and compare the severity of PTE using  $H_{LPBV}$  types with other factors suggesting the IPC burden, the S-type was assumed as 0, G-type as 1 and A-type as 2, in this study. If there was any disagreement in the data analysis, the final pattern of  $H_{LPBV}$  was obtained based on the consensus agreement between two readers. The interval between the first and secondary evaluations of the  $H_{LPBV}$  values was approximately four weeks. The mean and standard deviation (SD) of the  $H_{LPBV}$  values were also calculated using the workstation.

### Statistical analysis

Quantitative variables are expressed as mean±SD. The differences in patient characteristics and CT measurements with normally and non-normally distributed variables were determined based on the presence of PTE with the Student t and Mann-Whitney tests. Categorical variables were compared by using the Fisher exact

test. Spearman's rank and Pearson correlation coefficients between quantitative results of LPBV ( $H_{LPBV}$ ,  $V_{s'}$  and  $\%V_{s'}$ ) and the various factors suggesting of the severity of the pulmonary embolic burden were analyzed, including the ejection fraction (EF; %) and estimated systolic PA pressure (ePAP; mmHg) using echocardiography, the short-axis RV diameters, RV/LV diameter ratio, PA diameter, PA/Ao diameter ratio and CTOI using the same statistical software program used to perform the calculations, SPSS for Windows, release 19.0 (SPSS, IBM Inc.). Based on three types of  $H_{LPBV}$  the patients' characteristics and CT measurements were evaluated using one-way ANOVA followed by Tukey honestly significant difference (HSD) test for normally distributed variables and Kruskal-Wallis test followed by Mann-Whitney U test with Bonferroni correction to identify pairs of significantly different groups.

The inter-reader and intrareader agreement for determining the  $H_{LPBV}$  pattern was calculated based on the kappa statistic between the two readers. The strength of agreement was interpreted as poor (<0.20), fair (0.21–0.40), moderate (0.41–0.60), good (0.61–0.80), or excellent (0.81–0.99) (15).

## Results

The patients' clinical characteristics and CT measurements were summarized in Table 1 based on the presence of PTE. There were no significant differences in patient age, gender, body mass index (BMI, kg/m<sup>2</sup>) or EF. However, the ePAP on echocardiography, D-dimer level and heart rate (HR, beats per minute: bpm) were significantly higher in patients with PTE ( $P < 0.001$ ). CT measurements suggesting right heart strain, including  $V_{s'}$ ,  $\%V_{s'}$ , RV diameter, RV/LV diameter ratio, and  $H_{LPBV}$  pattern, were significantly greater in patients with PTE (Table 1).

The  $H_{LPBV}$  analysis showed that there were PTEs in all 12 patients with A-type pattern (100%), 19 of 25 patients with G-type pattern (76.0%) and 24 of 131 patients with S-type pattern (18.3%), as shown in Table 2. The D-dimer levels and quantitative CT values of  $V_{s'}$ ,  $\%V_{s'}$ , RV diameter, RV/LV diameter ratio and PA/Ao diameter ratio were significantly higher in patients with G-type and A-type pattern than in patients with S-type pattern (Table 2). Based on  $H_{LPBV}$  there were significant differences in D-dimer level, EF, ratio of IPCs,  $V_{s'}$ ,  $\%V_{s'}$ , RV diameter, and RV/LV diameter ratio.

The diagnostic performance of histogram pattern analysis for the detection of

**Table 1.** Patients' characteristics and CT measurements based on the presence of PTE

	All patients (n=168)	PTE (-) (n=113)	PTE (+) (n=55)	P
	Mean±SD (range)	Mean±SD	Mean±SD	
Males, n (%)	55 (32.1%)	31%	34.6%	0.73 <sup>a</sup>
Age (years)	62.9±16.8 (27–87)	63.4±15.8	62.0±18.7	0.64 <sup>b</sup>
BMI (kg/m <sup>2</sup> )	23.0±4.2 (17.2–39.2)	23.0±4.1	23.0±4.3	0.95 <sup>b</sup>
Ejection fraction (%)	66.3±9.7 (38–80)	66.7±10.4	65.9±9.1	0.74 <sup>b</sup>
ePAP (mmHg)	34.2±15.6 (15–95)	29.2±12.1	39.6±17.3	<0.001 <sup>b</sup>
D-dimer (mg/L)	13.9±27.5 (0.6–250.8)	9.1±12.7	23.5±42.7	<0.001 <sup>b</sup>
Heart rate (bpm)	81.9±16.5 (50–150)	78.8±13.3	87.7±20.0	<0.001 <sup>b</sup>
V <sub>120</sub> (mL)	2439.0±848.4 (410.1–4323)	2510.6±784.8	2291.7±957.0	0.14 <sup>c</sup>
V <sub>5</sub> (mL)	32.1±33.7 (1.4–199.6)	22.0±16.8	52.8±47.8	<0.001 <sup>b</sup>
%V <sub>5</sub> (%)	1.33±1.57 (0.15–14.4)	0.83±0.17	2.36±2.34	<0.001 <sup>b</sup>
H <sub>LPBV</sub> pattern	0.30±0.57 (0–2)	0.09±0.29	0.75±0.73	<0.001 <sup>b</sup>
RV diameter (mm)	35.3±7.6 (17.6–56.4)	33.9±7.0	38.1±7.9	0.001 <sup>c</sup>
RV/LV diameter ratio (%)	0.92±0.26 (0.34–2.38)	0.87±0.16	1.05±0.33	<0.001 <sup>b</sup>
PA/Ao diameter ratio (%)	0.88±0.17 (0.55–1.7)	0.87±0.16	0.92±0.19	0.08 <sup>b</sup>
CTDI of DECT	7.85±1.83 (4.96–12.26)	7.68±1.82	8.20±1.82	0.08 <sup>c</sup>
DLP of DECT	249.5±66.0 (127–416)	244.9±65.9	258.9±65.9	0.20 <sup>c</sup>
CTDI of CTV	10.85±2.48 (5.37–18.42)	10.5±2.3	11.6±2.6	0.009 <sup>c</sup>
DLP of CTV	1271.2±316.9 (612–2139)	1267.5±301.1	1278.8±349.9	0.83 <sup>c</sup>

CT, computed tomography; PTE, pulmonary thromboembolism; SD, standard deviation; BMI, body mass index; ePAP, estimated pulmonary artery pressure (systolic); V<sub>120</sub>, the volumetric value of lung pulmonary blood volume (PBV) ranging from 1 to 120 HU; V<sub>5</sub>, the volumetric value of lung PBV ranging from 1 to 5 HU; %V<sub>5</sub>, the ratio of V<sub>5</sub>/V<sub>120</sub>; H<sub>LPBV</sub>, histogram of lung PBV; RV, right ventricular; LV, left ventricular; PA, pulmonary artery; Ao, aorta; CTDI, CT dose index; DECT, dual energy CT; DLP, dose-length product; CTV, CT venography scanned using 100kV or 120kV.

<sup>a</sup>Fisher exact test; <sup>b</sup>Mann-Whitney U test; <sup>c</sup>Student's t test.

PTE was evaluated, and when the G- and A-type patients were thought to have PTEs, the sensitivity, specificity, positive predictive value (PPV), negative predictive value (NPV) and predictive accuracy were 56.4%, 92.9%, 83.8%, 87.6%, and 81.0%, respectively (Table 3). These values were superior to those of V<sub>5</sub> and %V<sub>5</sub>, except for sensitivity (Table 3). The H<sub>LPBV</sub> patterns and %V<sub>5</sub> values showed higher area under the curve (AUC) values (AUC, 0.76–0.81) than that of V<sub>5</sub> (0.72) based on presence of PTE (*P* < 0.001). In patients with PTE, the correlations with the factors suggesting the severity of PTE and DECT quantitative values of H<sub>LPBV</sub>, V<sub>5</sub> and %V<sub>5</sub> showed that %V<sub>5</sub> had the best correlations with ePAP (*r*=0.41; *P* = 0.03), RV diameter (*r* = 0.37; *P* < 0.001) and RV/LV diameter ratio (0.51; *P* < 0.001) (Table 4). However, the H<sub>LPBV</sub> pattern itself had good correlations with RV/LV diameter ratio (*r*=0.36; *P* = 0.007) and CTOI (*r*=0.63, *P* < 0.001).

To assess inter- and intrareader variability coefficient of variation for the H<sub>LPBV</sub> classification between two readers were analyzed, and good agreement was found, with high kappa values ranging from 0.79 to 0.87 in the inter-reader agreement and 0.84 to 0.93 in the intrareader agreement.

CT dose index (CTDI; mGy) and dose length product (DLP; mGycm) of DECT and CT venography are listed in Table 1. There were no significant differences in CTDI and DLP of DECT, but CTDI of CT venography was slightly larger in patients with PTE.

## Discussion

The LPBV using DECT provides fine CTPA, high-resolution lung CT image and additional perfusion information at a single examination (16) and displays decreased attenuation area caused by PTE (17, 18). However, the injection rate and the iodine

concentration of the contrast material affect the iodine perfusion maps (10). The quantification of LPBV depicts the severity of PTE and/or the pulmonary embolic burden (8, 18). In addition, the method used to inject the contrast material and scan time of LPBV also affect the absolute and relative values of LPBV (10). Nevertheless, the morphologic information regarding the presence of PTE and functional information of lung perfusion impairment can be obtained in one examination using a dual-energy technique (9), and quantitative evaluations of PTE using LPBV indicate the degree of pulmonary perfusion when determined using a workstation (14). However, the variation of injection rate of contrast material or scan timing also affects the quantitative evaluation of DECT images. To standardize the quantification of DECT in various conditions, gross evaluation of DECT using histo-

**Table 2.** Patients' characteristics and CT measurements based on histogram type

	S type (n=131)	G type (n=25)	A type (n=12)	P *	S vs. G	S vs. A	G vs. A
	mean±SD	mean±SD	mean±SD				
Gender (% male)	32.8%	40.0%	8.3%	0.054 <sup>a</sup>			
Age (years)	64.0±15.3	58.5±20.5	60.9±23.0	0.65 <sup>b</sup>			
BMI (kg/m <sup>2</sup> )	23.2±4.0	21.8±4.6	23.2±4.8	0.13 <sup>b</sup>			
Ejection fraction (%)	68.1±7.8	59.6±12.5	70.2±7.0	0.003 <sup>a</sup>	0.02	0.48	0.04
ePAP (mmHg)	31.7±15.9	37.8±16.4	39.8±11.9	0.24 <sup>c</sup>			
D-dimer (mg/L)	9.9±13.1	26.3±49.4	31.2±56.5	0.003 <sup>b</sup>	0.002	0.001	0.80
Heart rate (bpm)	80.1±14.6	86.9±23.0	88.9±16.1	0.08 <sup>b</sup>			
Ratio of IPCs (%)	18.3%	76%	100%	<0.001 <sup>a</sup>	<0.001	<0.001	0.011
V <sub>120</sub> (mL)	2510.5±781.7	2231.7±1055.1	2089.3±993.5	0.11 <sup>c</sup>			
V <sub>5</sub> (mL)	24.0±19.4	51.9±50.9	79.0±55.8	<0.001 <sup>b</sup>	0.012	0.006	0.15
%V <sub>5</sub> (%)	0.91±0.58	2.39±2.95	3.74±1.89	<0.001 <sup>b</sup>	0.02	<0.001	0.16
RV diameter (mm)	34.5±7.0	37.4±9.4	40.0±7.4	0.02 <sup>c</sup>	0.16	0.04	0.57
RV/LV diameter ratio (%)	0.87±0.17	1.02±0.42	1.21±0.34	<0.001 <sup>c</sup>	0.02	<0.001	0.07
PA/Ao diameter ratio (%)	0.87±0.16	0.94±0.23	0.93±0.13	0.07 <sup>b</sup>			

CT, computed tomography; S, symmetric; G, gradual; A, asymmetric; SD, standard deviation; BMI, body mass index; ePAP, estimated pulmonary artery pressure (systolic); IPC, intrapulmonary clot; V<sub>120</sub>, the volumetric value of lung pulmonary blood volume (PBV) ranging from 1 to 120 HU; V<sub>5</sub>, the volumetric value of lung PBV ranging from 1 to 5 HU; %V<sub>5</sub>, the ratio of V<sub>5</sub>/V<sub>120</sub>; RV, right ventricular; LV, left ventricular; PA, pulmonary artery; Ao, aorta.

<sup>a</sup>Fisher exact test; <sup>b</sup>Kruskal-Wallis test followed by Mann-Whitney U test; <sup>c</sup>One-way ANOVA with post-hoc Tukey HSD test.

**Table 3.** The diagnostic performance of H<sub>LPBV</sub>, V<sub>5</sub> and %V<sub>5</sub> based on the presence of intrapulmonary clots

	H <sub>LPBV</sub>	V <sub>5</sub>	%V <sub>5</sub>
Cutoff value	1.0	50.0	2.2
True-positive finding	31	32	38
True-negative finding	105	84	94
False-positive finding	6	29	19
False-negative finding	24	23	17
Accuracy (%)	81.0	69.0	78.6
Sensitivity (%)	56.4	58.2	69.1
Specificity (%)	92.9	74.3	83.2
Positive predictive value (%)	83.8	52.5	66.7
Negative predictive value (%)	87.6	78.5	84.7
AUC	0.76	0.72	0.81

H<sub>LPBV</sub>, histogram pattern of lung pulmonary blood volume (LPBV); V<sub>5</sub>, the volumetric value of LPBV ranging from 1 to 5 HU; %V<sub>5</sub>, the ratio of V<sub>5</sub>/V<sub>120</sub>; AUC, area under the curve.

tively, and the highest specificity, PPV and NPV were achieved in H<sub>LPBV</sub> out of these volumetric values of LPBV. In most patients without PTE, DECT showed a symmetric histogram of LPBV, but further classifications of histogram pattern were necessary, compared with V<sub>5</sub> and %V<sub>5</sub> (Table 3).

Compared with the findings of a previous study using relative volumetric values of LPBV (AUC of %V<sub>5</sub>: 0.73) based on the presence of PTE (17), the AUCs for H<sub>LPBV</sub> and %V<sub>5</sub> were slightly higher in this study. However, the H<sub>LPBV</sub> pattern demonstrated lower correlations with factors suggesting the severity of PTE, such as ePAP (r=0.18), heart rate (r=0.09), RV diameter (r=0.16), the RV/LV diameter ratio (r=0.36) than those of V<sub>5</sub> and %V<sub>5</sub>. These low correlations between H<sub>LPBV</sub> patterns and the factors indicating PTE severity might be due to the limited histogram pattern ranging from 0 to 2 (Table 4). However, in patients with PTEs, the CTOI score showed a good correlation with the H<sub>LPBV</sub> pattern (r=0.63, P < 0.001), similar to the %V<sub>5</sub> (r=0.64). The severity of PA obstruction can be used as an indicator of the hemodynamic severity of PTE (13); however, discrepancies regarding the potential association between

gram-pattern analysis might be one of solution to diagnose PTE. In this study, when the S-type H<sub>LPBV</sub> pattern was considered negative and G- and A-type H<sub>LPBV</sub> patterns

were considered positive for the presence of PTE, the sensitivity, specificity, PPV, NPV and predictive accuracy were 56.4%, 92.9%, 83.8%, 87.6% and 81.0% (Table 3), respec-

**Table 4.** The correlation between the  $H_{LPBV}$  pattern,  $V_s$ ,  $\%V_s$  and the factor suggesting the severity of PTE (n=55)

	$H_{LPBV}$		$V_s$		$\%V_s$	
	r	P	r	P	r	P
Ejection fraction (%)	0.01	0.97 <sup>a</sup>	-0.01	0.97 <sup>a</sup>	0.06	0.75 <sup>a</sup>
ePAP (mmHg)	0.18	0.34 <sup>a</sup>	0.37	0.05 <sup>a</sup>	0.41	0.03 <sup>a</sup>
Heart rate (bpm)	0.09	0.52 <sup>a</sup>	-0.29	0.03 <sup>a</sup>	-0.11	0.41 <sup>a</sup>
RV diameter (mm)	0.16	0.26 <sup>b</sup>	0.30	0.03 <sup>b</sup>	0.37	0.005 <sup>b</sup>
RV/LV diameter ratio (%)	0.36	0.007 <sup>b</sup>	0.43	<0.001 <sup>b</sup>	0.51	<0.001 <sup>b</sup>
CTOI	0.63	<0.001 <sup>a</sup>	0.49	<0.001 <sup>a</sup>	0.64	<0.001 <sup>a</sup>

PTE, pulmonary thromboembolism;  $H_{LPBV}$ , histogram pattern of LPBV;  $V_s$ , the volumetric value of LPBV ranging from 1 to 5 HU;  $\%V_s$ , the ratio of  $V_s / V_{120}$ ; ePAP, estimated pulmonary artery pressure (systolic); RV, right ventricular; LV, left ventricular; CTOI, computed tomography obstruction index.

<sup>a</sup>Spearman's rank correlation coefficient; <sup>b</sup>Pearson correlation coefficient.

the severity of CTOI and the immediate outcome are shown due to differences in studied populations in terms of PTE severity (12, 13, 16). The  $\%V_s$  value represents the relative value of the lower perfusion volume on DECT and demonstrates correlations with factors suggesting the severity of PTE (8), whereas the  $H_{LPBV}$  pattern is thought to grossly indicate the whole pulmonary perfusion, despite the effects of different contrast conditions, including injection rate or total iodine volume. Meanwhile, the CTOI score does not take into account the presence of clots in small peripheral PAs, and the PA clot load score is restricted to the segmental or subsegmental PAs. In contrast, DECT provides both morphologic CTPA images and functional images of contrast distribution in the lung parenchyma.

This study has several limitations. First, it was performed at a single center, and the study population was small; therefore, our results are preliminary and further evaluations are needed. Second, the beam hardening artifact-related focal iodine defects without relation to PTE are detected in the upper lobe or medial segment of middle lobes on DECT (19) and may affect the histogram pattern of LPBV. In order to minimize contrast-related beam-hardening artifacts, caudocranial scans and a higher injection rate of iodine contrast-material may be employed to obtain the best image quality for both CTPA and perfusion map images of the lungs due to the high attenuation in the PAs (10). Third, the coverage using the small FOV (260 mm) is not feasible for the whole lung analysis. The solution to this problem is to position the

patient exactly in the center of the gantry to keep the patient's lungs inside the area covered by both tubes. Fourth, comorbid pulmonary diseases, such as pulmonary emphysema (20), also influence the quantification of the LPBV (21). In patients with pulmonary emphysema, the lower attenuation area on lung CT correlated with that on DECT (21) and might affect the quantification of DECT or histogram analysis, and the patients with pulmonary emphysema were excluded from this study. Fifth, the  $H_{LPBV}$  patterns were divided into only three types based on our experience; however, the sensitivity (56.4%), PPV (83.8%), and predictive accuracy (81.0%) were not high, thus further classification of the  $H_{LPBV}$  patterns is needed. The gradual or bumpy up-slopes may be divided into additional subgroups which would improve the sensitivity and/or diagnostic accuracy based on the presence of the PTE. The last problem is radiation exposure. CTDI of DECT was smaller than that of CT venography (Table 1), and DECT is feasible for routine examination without additional dose or compromises in image quality (22). The CTDI of CT venography was larger in patients with PTE, because the leg edema was caused by intravenous thrombus. However, further attention to radiation exposure should be paid for radiation exposure of DECT and CT venography.

In conclusion, the results of this preliminary study demonstrate that  $H_{LPBV}$  analyses may be applied to obtain a diagnosis of pulmonary thromboembolism. In patients with a symmetric  $H_{LPBV}$  pattern, the possibility of PTE was low on CTPA, and the gradual and bumpy up-slopes for the  $H_{LPBV}$  values

predominantly indicated the presence of pulmonary artery filling defects, with high specificity (92.9%) and NPV (87.6%). However, further evaluations and classification based on the histogram pattern will be needed in order to improve the sensitivity and predictive accuracy.

#### Conflict of interest disclosure

The authors declared no conflicts of interest.

#### References

- Horlander KT, Mannino DM, Leeper KV. Pulmonary embolism mortality in the United States, 1979-1998: an analysis using multiple-cause mortality data. *Arch Intern Med* 2003; 163:1711-1717. [CrossRef]
- Chae EJ, Seo JB, Jang YM, et al. Dual-energy CT for assessment of the severity of acute pulmonary embolism: pulmonary perfusion defect score compared with CT angiographic obstruction score and right ventricular/left ventricular diameter ratio. *AJR Am J Roentgenol* 2010; 194:604-610. [CrossRef]
- Bauer RW, Frellesen C, Renker M, et al. Dual-energy CT pulmonary blood volume assessment in acute pulmonary embolism - correlation with D-dimer level, right heart strain and clinical outcome. *Eur Radiol* 2011; 21:1914-1921. [CrossRef]
- Kim BH, Seo JB, Chae EJ, et al. Analysis of perfusion defects by causes other than acute pulmonary thromboembolism on contrast-enhanced dual-energy CT in consecutive 537 patients. *Eur J Radiol* 2012; 81:e647-e652. [CrossRef]
- Sueyoshi E, Tsutsui S, Hayashida T, et al. Quantification of lung perfusion blood volume (lung PBV) by dual-energy CT in patients with and without pulmonary embolism: Preliminary results. *Eur J Radiol* 2011; 80:e505-e509. [CrossRef]
- Remy-Jardin M, Pistolesi M, Goodman LR, et al. Management of suspected acute pulmonary embolism in the era of CT angiography: a statement from the Fleischner Society. *Radiology* 2007; 245:315-329. [CrossRef]
- Zhang LJ, Chai X, Wu SY, et al. Detection of pulmonary embolism using dual-energy computed tomography and correlation with cardiovascular measurements: a preliminary study. *Acta Radiol* 2009; 50:892-901. [CrossRef]
- Okada M, Nakashima Y, Kunihiro Y, et al. Volumetric evaluation of dual-energy perfusion CT for the assessment of intrapulmonary clot burden. *Clin Radiol* 2013; 68:e669-e675. [CrossRef]
- Sakamoto A, Sakamoto I, Nagayama H, et al. Quantification of lung perfusion blood volume with dual-energy CT: assessment of the severity of acute pulmonary thromboembolism. *AJR Am J Roentgenol* 2014; 203:287-291. [CrossRef]
- Nance JW, Jr, Henzler T, Meyer M, et al. Optimization of contrast material delivery for dual-energy computed tomography pulmonary angiography in patients with suspected pulmonary embolism. *Invest Radiol* 2012; 47:78-84. [CrossRef]
- Pagnamenta A, Vanderpool R, Brimioule S, et al. Proximal pulmonary arterial obstruction decreases the time constant of the pulmonary circulation and increases right ventricular afterload. *J Appl Physiol* 2013; 114:1586-1592. [CrossRef]

12. Pruszczyk P, Torbicki A, Pacho R, et al. Noninvasive diagnosis of suspected severe pulmonary embolism: transesophageal echocardiography vs spiral CT. *Chest* 1997; 112:722–728. [\[CrossRef\]](#)
13. Qanadli SD, El Hajjam M, Vieillard-Baron A, et al. New CT index to quantify arterial obstruction in pulmonary embolism: comparison with angiographic index and echocardiography. *AJR Am J Roentgenol* 2001; 176:1415–1420. [\[CrossRef\]](#)
14. Johnson TR, Krauss B, Sedlmair M, et al. Material differentiation by dual energy CT: initial experience. *Eur Radiol* 2007; 17:1510–1517. [\[CrossRef\]](#)
15. Eliasziw M, Young SL, Woodbury MG, et al. Statistical methodology for the concurrent assessment of interrater and intrarater reliability: using goniometric measurements as an example. *Phys Ther* 1994; 74:777–788. [\[CrossRef\]](#)
16. Thieme SF, Johnson TR, Lee C, et al. Dual-energy CT for the assessment of contrast material distribution in the pulmonary parenchyma. *AJR Am J Roentgenol* 2009; 193:144–149. [\[CrossRef\]](#)
17. Okada M, Nakashima Y, Kunihiro Y, et al. Volumetric evaluation of dual-energy perfusion CT by the presence of intrapulmonary clots using a 64-slice dual-source CT. *Act Radiol* 2013; 54:628–633. [\[CrossRef\]](#)
18. Meinel FG, Graef A, Bamberg F, et al. Effectiveness of automated quantification of pulmonary perfused blood volume using dual-energy CTPA for the severity assessment of acute pulmonary embolism. *Invest Radiol* 2013; 48:563–569. [\[CrossRef\]](#)
19. Kang MJ, Park CM, Lee CH, et al. Focal iodine defects on color-coded iodine perfusion maps of dual-energy pulmonary CT angiography images: a potential diagnostic pitfall. *AJR Am J Roentgenol* 2010; 195:W325–W330. [\[CrossRef\]](#)
20. Meinel FG, Graef A, Sommer WH, et al. Influence of vascular enhancement, age and gender on pulmonary perfused blood volume quantified by dual-energy-CTPA. *Eur J Radiol* 2013; 82:1565–1570. [\[CrossRef\]](#)
21. Okada M, Kunihiro Y, Nakashima Y, et al. The low attenuation area on dual-energy perfusion CT: correlation with the pulmonary function tests and quantitative CT measurements. *Eur J Radiol* 2012; 81:2892–2899. [\[CrossRef\]](#)
22. Schenzle JC, Sommer WH, Neumaier K, et al. Dual energy CT of the chest: how about the dose? *Invest Radiol* 2010; 45:347–353. [\[CrossRef\]](#)